Journal of Chemical Technology and Metallurgy, 59, 5, 2024, 1119-1129

SONOCHEMICAL SYNTHESIS OF SILVER NANOPARTICLES FOR GAS-DIFFUSION ELECTRODES APPLICATION

Borislava Mladenova[1], Toma Stankulov[1], Simeon Stankov[1], Maria Karsheva[†2],
Ivaylo Hinkov[2], Anton Momchilov[1], Reneta Boukoureshtlieva[1]

[1]Institute of Electrochemistry and Energy Systems "Acad. Evgeni Budevski"
Bulgarian Academy of Sciences, Acad. Georgi Bonchev St.
Block 10, Sofia 1113, Bulgaria
[2]Department of Chemical Engineering
University of Chemical Technology and Metallurgy
8 St. Kliment Ohridsky Blvd., Sofia 1797, Bulgaria
E-mail: borislava.mladenova@iees.bas.bg

Received 13 October 2023
Accepted 25 June 2024
DOI: 10.59957/jctm.v59.i5.2024.14

ABSTRACT

The aim of the current study is to explore the application of silver nanoparticles (AgNPs) as a catalyst in air gas-diffusion electrodes (AGDE). AgNPs have been successfully synthesized through an original sonochemical method. The effects of reagent concentrations, temperature and reaction time were studied as well. Composites of AgNPs and activated carbon (Norit NK) were prepared by using two adsorption methods to demonstrate the catalytic activity. Method 1 involves homogenizing preliminary prepared AgNPs colloid solution and Norit NK followed by evaporation of the suspension. One-step route was used for Method 2, i.e. all components were mixed altogether and sonicated, resulting in the AgNPs formation directly on the surface and inside the pores of Norit NK. Additionally, some of the samples were thermally treated at 300°C for 1h under air and argon. The composites were characterized by X-ray diffraction (XRD), scanning electron microscopy with energy dispersive X-Ray analysis (SEM/EDX) and transmission electron microscopy (TEM). The catalytic activity of the obtained composites regarding oxygen reduction reaction (ORR) was investigated in AGDE using an aqueous 4M NaCl electrolyte. The thermally treated composite obtained via Method 2 appears to show improved electrochemical catalytic activity regarding ORR in comparison to the Method 1 samples.

Keywords: air gas-diffusion electrode, oxygen reduction reaction, silver nanoparticles, sonochemical synthesis.

INTRODUCTION

The development of renewable energy sources and storage systems is fundamental for the future economic, social and eco-oriented progress of humankind. Metal-air systems, which fuse features of batteries and fuel cells, are of particular interest due to their high energy density, safety and finally use of oxygen from the air. The major challenge of these systems is to achieve a balance between maximum catalytic activity and minimum cost of catalysts, being in most of the cases precious metals. Silver has been studied as a potential substitute for platinum due to its high catalytic activity for electrochemical reduction of oxygen and the decomposition of hydrogen peroxide, lower cost and wider distribution. These properties make Ag an attractive candidate for a catalyst in air electrodes for alkaline fuel cells (AFC) and metal-air batteries, in its pure form or binary/ternary nano-alloys (Ag-Cu, Ag-Pd, Ag-Au, Ag-Co etc.) [1]. A commonly used approach is the preparation of composite which consists of a small amount of catalyst and carbon material (support substrate) such as activated carbon [2 - 4], carbon paper [5], carbon nanotubes [6, 7], etc. Yang et al. investigated silver-carbon composite materials prepared via functional ion pre-adsorption method obtaining Ag with different particle-size and morphology

[3]. Modified multi-walled carbon nanotubes and Ag composites were prepared using in-situ growth method [7]. Carbon-supported silver catalysts consisting of different Ag amounts were prepared by a citrate-protecting method [4]. P. Singh et al. reported electrodes prepared using "bare" silver (substrate-free) via the Layer by Layer method [8]. Electrochemical deposition under potentiostatic and galvanostatic modes were used to ensure uniform distribution of the catalyst on the top of the gas diffusion support [2, 5]. Silver nanoparticles (AgNPs) were successfully implemented as a substitute for the Pt catalysts in a variety of electrochemical systems such as alkaline fuel cells, direct methanol fuel cells (MFCs) [1, 5], zinc-air battery [6], oxygen cathodes to practical chlor-alkali electrolysis [9], antimicrobial agents in MFCs [2], etc.

Different chemical, physical and biological methods were employed for the preparation of silver nanoparticles such as chemical vapor deposition and atomic layer deposition [10], electrochemical [11, 12] and sonoelectrochemical synthesis [13], photoreduction [14], laser ablation [15], microwave-assisted techniques [16], ultrasonic irradiation [17], Tollens method [18] etc. Depending on the synthesis approach, AgNPs of different size and morphology (nanospheres [19], multi-branched flowers [20], nanobars [21] and nanocubes [22, 23]) were obtained. However, the chemical reduction in aqueous solutions is one of the most frequently used approaches for AgNPs synthesis. $AgNO_3$ [24] or AgCl [25] are usually used as silver precursors while ethanol [26], sodium citrate [27], sodium borohydride [28], ascorbic acid [29] are employed as reducing agents. Recently, sonochemistry was introduced as an environmentally benign approach for the preparation of silver nanoparticles. This method offers milder conditions, shorter reaction times, and higher yields in comparison to the conventional chemical reduction methods [30].

In the present work, we investigate the catalytic activity of silver nanoparticles obtained via chemical reduction using sonication. AgNPs were integrated onto the active layer of AGDE to demonstrate their catalytic activity. Two different methods of silver nanoparticles and Norit NK activated carbon composites preparation were developed. The electrodes' catalytic activity was studied in three electrode half-cell with Ag/AgCl reference electrode using 4M NaCl solution as electrolyte.

EXPERIMENTAL

Synthesis of silver nanoparticles (AgNPs)

Analytically grade silver nitrate (> 99.8 % $AgNO_3$, Sigma-Aldrich) was dissolved in distilled water by vigorously stirring at room temperature. Afterwards, 0.8 mL C_2H_5OH (96 %, Valerus Co., Bulgaria) and 0.8 mL 25 % NH_4OH solution (Valerus Co., Bulgaria) were added drop-wise to the solution. The total volume of the solutions was constantly kept at 100 mL. Then, the solution was sonicated in an ultrasonic bath (UST 2.8 - 100, 32 kHz, Siel Ltd., Bulgaria). The syntheses were performed at two temperatures (30 and 50°C) of the ultrasonic bath media.

Air gas-diffusion electrodes

The AGDE were composed of gas-supplying (100 mg cm^{-2}) and catalytic (20 mg cm^{-2}) layers (Fig. 1). The hydrophobic gas-supplying layer was made of teflonized acetylene black (XC35) which was prepared by using acetylene black (P1042) and polytetrafluoroethylene (PTFE) following a similar preparation approach to the reported by Iliev et al. [31]. The catalytic layer was prepared by mixing composite material (Ag-activated carbon) and XC35 in 2:1 ratio, respectively. A stainless-steel mesh was used as a supporting matrix and current collector. Two preparation methods of Ag-Norit NK composites were developed.

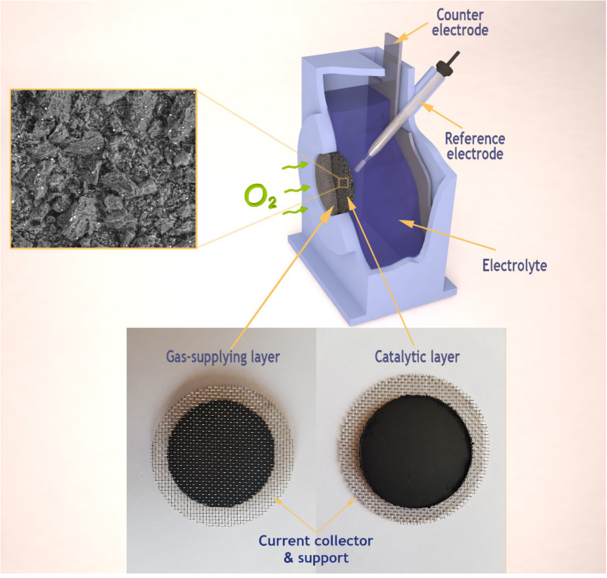

Fig. 1. Three-dimensional model of the test cell.

Method 1

An activated carbon Norit NK (NORIT, Amersfoort, Netherlands) was added to preliminary prepared colloids of silver nanoparticles obtained from 4, 5 and 6 mmol L^{-1} $AgNO_3$ solutions. The mixtures were constantly stirred and evaporated at 80°C (IKA RH basic KT/C stirrer equipped with IKA ETS-D5 thermocouple, Germany) until the liquid was almost completely removed. Further, the wet composites were dried in an oven at 100°C for 24 h under air atmosphere. The samples were denoted as M1US4 (4 mmol L^{-1} $AgNO_3$ solution and Norit NK), M1US5 (5 mmol L^{-1} $AgNO_3$ solution and Norit NK) and M1US6 (6 mmol L^{-1} $AgNO_3$ solution and Norit NK). Additionally, other samples prepared in the same manner were heated at 300°C for 1 hour. The resulting composites were designated as M1TA4 (4 mmol L^{-1} solution and Norit NK), M1TA5 (5 mmol L^{-1} $AgNO_3$ solution and Norit NK) and M1TA6 (6 mmol L^{-1} $AgNO_3$ solution and Norit NK). Another composite sample (M1TAr5), obtained from 5 mmol L^{-1} $AgNO_3$, was thermally treated under argon instead of air atmosphere at 300°C for 1 h to explore possible oxidation of the AgNPs during the thermal treatment as a detrimental factor of the AGDE catalytic activity.

Method 2

$AgNO_3$ (5 mmol L^{-1}) was dissolved in 100 mL distilled water. After complete dissolution of the silver nitrate, 0.8 mL 96 % C_2H_5OH, 0.8 mL 25 % NH_4OH and 2.55 g Norit NK were added to the solution in the respective order. Then the mixture was sonicated in ultrasonic bath. After sonication, the samples were evaporated at constantly stirring, followed by drying in the same manner as described for Method 1. The untreated sample was denoted as M2US5. The other composite (M2TA5) was thermally treated for 1 h under air at 300°C analogically to Method1.

All samples obtained through both methods, the corresponding conditions and treatments are summarized in Table 1.

Characterization

The colloidal AgNPs solutions were analysed using a UV-Visible spectrophotometer (T60, PG Instruments Ltd., U.K.) immediately after synthesis. X-ray powder diffraction (XRD) data of the composites were collected on a Philips APD 15 diffractometer, using Cu Kα radiation (λ = 1.5418 Å). The morphology of the samples was examined by dual beam scanning electron microscope focused ion beam system (SEM/FIB LYRA I XMU, Tescan, Czech Republic), equipped with EDX detector (Quantax 200, Bruker, USA). Moreover, the morphology of the obtained silver nanoparticles from a solution and the composites was studied by Transmission Electron Microscopy on a JEOL JEM 2100, 80-200 kV (Jeol Ltd. Japan).

Electrochemical experiments were carried out in the half-cell conditions using 4M NaCl electrolyte, stainless steel as the counter electrode and a reference electrode Ag/AgCl (Fig. 1). The catalytic activity of air gas-diffusion electrodes was investigated via polarization curves recording.

Table 1. Summary of the methods and conditions for the preparation of the various Ag-Norit NK composites.

	Sample	$AgNO_3$ concentration in the solution, mmol L^{-1}	Drying process	Thermal treatment
Method 1	M1US4	4	100°C, 24 h, Air	-
	M1US5	5	100°C, 24 h, Air	-
	M1US6	6	100°C, 24 h, Air	-
	M1TA4	4	100°C, 24 h, Air	300°C, 1 h, Air
	M1TA5	5	100°C, 24 h, Air	300°C, 1 h, Air
	M1TA6	6	100°C, 24 h, Air	300°C, 1 h, Air
	M1TAr5	5	100°C, 24 h, Air	300°C, 1 h, Ar
Method 2	M2US5	5	100°C, 24 h, Air	-
	M2TA5	5	100°C, 24 h, Air	300°C, 1 h, Air

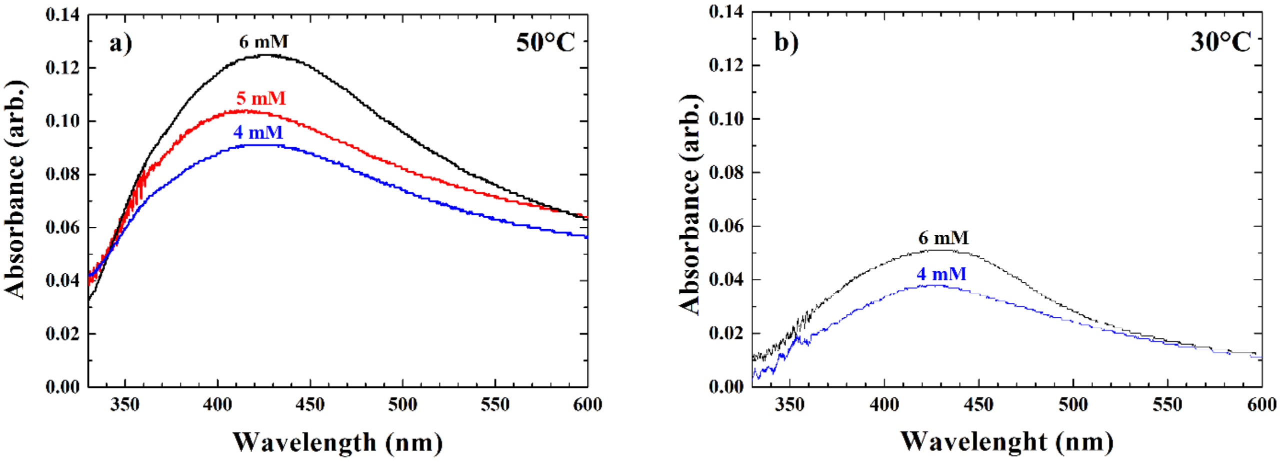

Fig. 2. UV-Vis spectra of AgNPs solutions prepared for 6 min. sonication: (a) 4, 5 and 6 mM $AgNO_3$ solutions at 50°C and (b) 4 mM and 6 mM $AgNO_3$ solutions at 30°C.

RESULTS AND DISCUSSION

Aqueous solutions of $AgNO_3$, C_2H_5OH and NH_4OH were prepared and sonicated for 6 minutes at two different bath media temperatures (30°C and 50°C). The colour of the solutions became light yellow indicating the formation of colloidal silver. The UV-Vis absorption spectra (Fig. 2) of all samples appear to show a peak at about 400 - 425 nm which is characteristic for spherical silver nanoparticles [14]. The absorbance intensity increases along with the increase of $AgNO_3$ concentration. There is a significant difference in the absorbance values of the solutions obtained at 50°C (Fig. 2a) and 30°C (Fig. 2b). This is most likely due to the slower kinetics of the chemical reaction at 30°C. It is important the ultrasonic bath media temperature to be kept equal or below 50°C to avoid oxidation of the AgNPs in the solution.

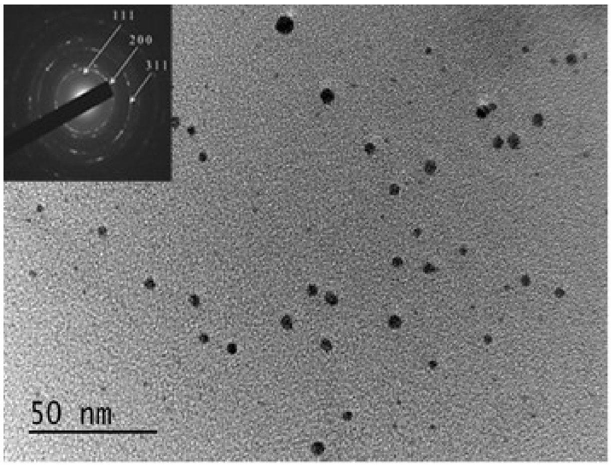

Fig. 3. TEM micrograph of a sample obtained from 6 mmol L^{-1} $AgNO_3$ solution at 50°C.

The morphology of AgNPs obtained from 6 mmol L^{-1} $AgNO_3$ solution at 50°C was observed by Transmission Electron Microscopy 24 hours after synthesis (Fig. 3). The sample exhibits nearly spherical-shaped particles. The particle size varies from 1 to 7 nm as the size distribution is predominantly in the range of 3 - 4 nm. The electron diffraction pattern (Fig. 3 inset) displays concentric rings of a face-centred cubic lattice (space group Fm-3m) with unit cell parameters a = b = c = 4.077 Å.

Fig. 4 shows the X-ray diffraction (XRD) patterns of composites (Norit NK active carbon and silver nanoparticles) obtained via Method 1 - untreated (Fig. 4a) and heated at 300°C for 1h in air atmosphere (Fig. 4b). Additionally, XRD data were collected for Norit NK as reference material. The data of all composites fitted well to the face-centred cubic structure (Fm-3m) of the Ag (ICSD 44387) [32]. An additional peak at 26.6 °2ϴ indicates presence of graphite (ICSD 52230) [33] in the Norit NK sample. There are also few unidentified peaks (marked with *) in the profiles of M1US5 (68.2 °2ϴ), M1TA5 (68.2 °2ϴ) and M1US6 (39.4 and 41.3 °2ϴ).

Polarization curves were plotted to evaluate the catalytic activity of the composites obtained via Method 1 (Fig. 5). Among the thermally untreated composites,

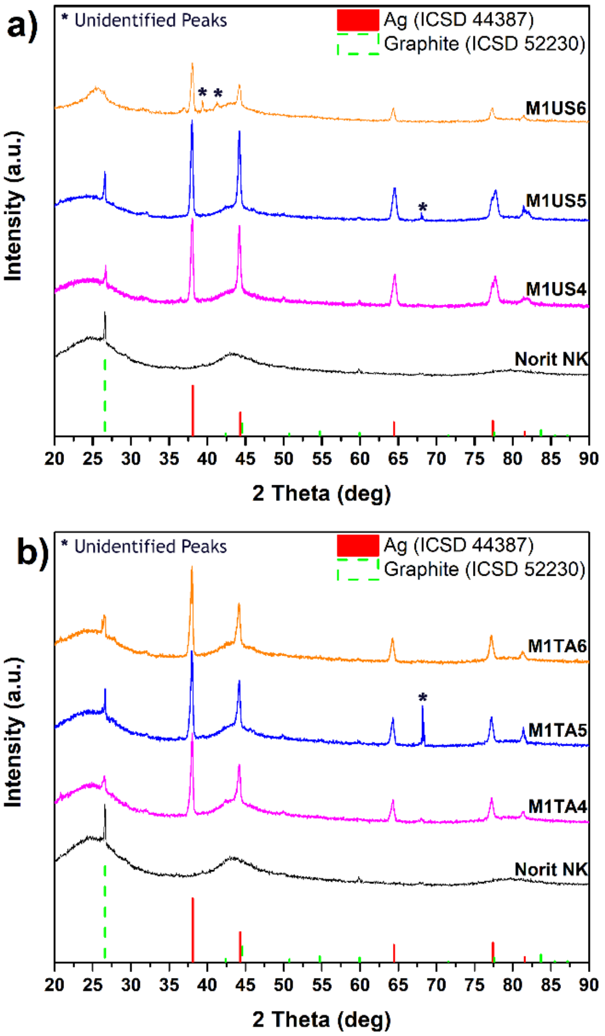

Fig. 4. X-ray powder diffraction profiles of activated carbon NoritNK and the composites prepared via Method 1: (a) untreated and (b) thermally treated.

the M1US5 electrode exhibits the lowest polarization while M1US6 marks the most noticeable potential drop in this group (Fig. 5a). The M1US6 behaviour could be attributed to the higher initial $AgNO_3$ concentration, which subsequently might lead to Ag agglomeration during the composite and electrode preparation resulting in less electrochemically active surface area hence detrimental for the sample performance. Similarly to M1US5, the thermally treated composite obtained from 5 mM $AgNO_3$ solution (M1TA5), appears to show better catalytic activity in comparison to the other samples in the thermally treated group (Fig. 5b).

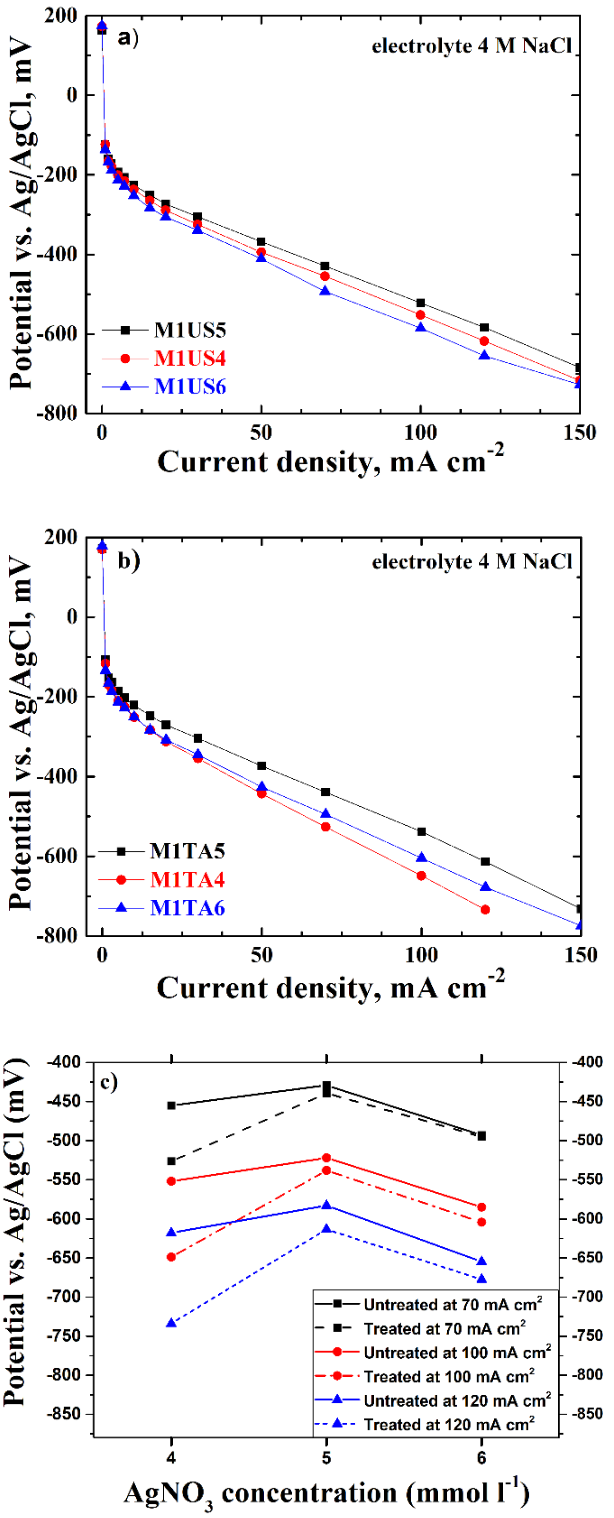

Fig. 5. Polarization curves of electrodes (a) non-thermally and (b) thermally treated composites; and (c) potential as a function of the composites' Ag concentration of the thermally untreated (solid lines) and treated (dashed lines) samples at current densities of 70 mA cm^{-2}, 100 mA cm^{-2} and 120 mA cm^{-2}.

A relationship between the potential and composites' Ag concentration was plotted to compare the two groups of samples at current densities of 70 mA cm^{-2}, 100 mA cm^{-2} and 120 mA cm^{-2} (Fig. 5c). Apparently, the untreated composites performed better compared to their treated counterparts in almost all cases. The more pronounced potential drop of the treated group could be explained by partial surface oxidation of the Ag particles during the composite thermal treatment. It is interesting to note that the differences in the potentials between untreated and treated samples became less evident with the increase of Ag content to the point that there is almost no difference in the potential values between M1US6 and M1TA6 at 70 mA cm^{-2}.

In order to confirm indirectly the oxidation as a cause for the worse electrochemical behaviour, we prepared a composite (M1TAr5) obtained from 5 mmol L^{-1} AgNO$_3$ solution, which was later heated at 300°C for 1h in argon instead of air atmosphere. This sample and untreated M1US5 resembles similar electrochemical behaviour to each other, confirming our assumption for the oxidation as a possible detrimental cause (Fig. 6). The growing difference in the polarization between these two samples and treated in air (M1TA5) is more evident at current densities higher than 50 mA cm^{-2}.

Considering the results of the composites obtained from 5 mmol L^{-1} AgNO$_3$ solution, we decided to prepare samples (M2US5 and M2TA5) with the same concentration in a single step (Method 2). M2TA5 sample was thermally treated under air in the same manner as Method 1.

The XRD patterns of M2US5 and M2TA5 composites (Fig. 7) exhibit slightly lower intensity of the Ag reflections (ICSD 44387) [32] in comparison to the composites prepared via Method 1. This phenomenon might be caused by a direct formation of Ag particles inside the activated carbon pores which walls may slightly prevent the x-rays penetration and/or absorb the reflected rays from the silver. It also seems that the graphite in Norit NK was transformed into amorphous carbon or some other allotropic form of carbon, evident by the absence of a peak at 26.6 °2Θ in the M2US5 and M2TA5 patterns. This phenomenon was most likely caused by the ultrasonic treatment.

The polarization curves of composites (obtained from 5 mmol L^{-1} AgNO$_3$ solutions) prepared via both methods (thermally treated and untreated) are compared in Fig. 8. The thermally treated sample

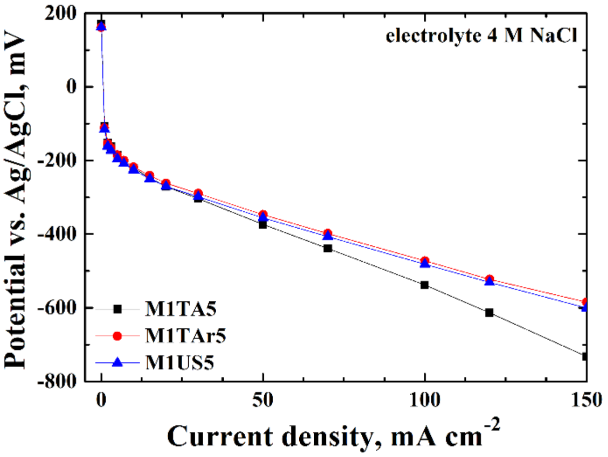

Fig. 6. Polarization curves of composites obtained from 5 mmol L^{-1} AgNO$_3$ solution – untreated (M1US5), thermally treated under argon (M1TAr5) and air (M1TA5).

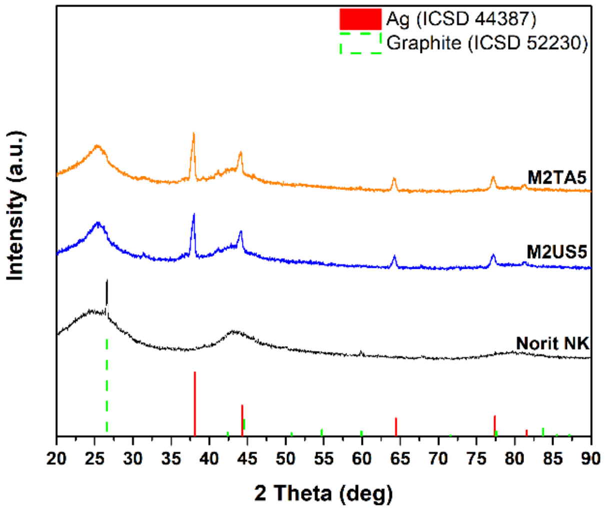

Fig. 7. X-ray powder diffraction profiles of composites prepared via Method 2.

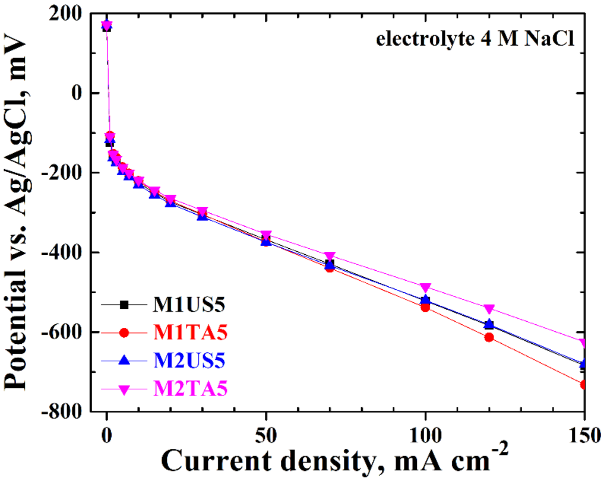

Fig. 8. Polarization curves of electrodes prepared via Method 1 and Method 2 (thermally and non-thermally treated).

prepared via Method 2 (M2TA5) seems to exhibit the lowest polarization among all examined samples. The performance of M1US5 and M2US5 is similar, slightly better in M2US5 case. Method 2 samples better electrochemical behaviour can be explained by the Ag formation inside the activated carbon pores, which might prevent the oxidation during the composite preparation and the following heating process.

The SEM images of these four samples (Fig. 9) show Norit NK's porous particles with irregular shapes, being from few micrometers to few hundred micrometers. The highly contrasting Ag particles (white spots) on the Norit NK surface appears to grow additionally during the composite preparation process in comparison to the observed AgNPs 24h after their synthesis in Fig. 3. It is also interesting to note that the Ag particles are seen

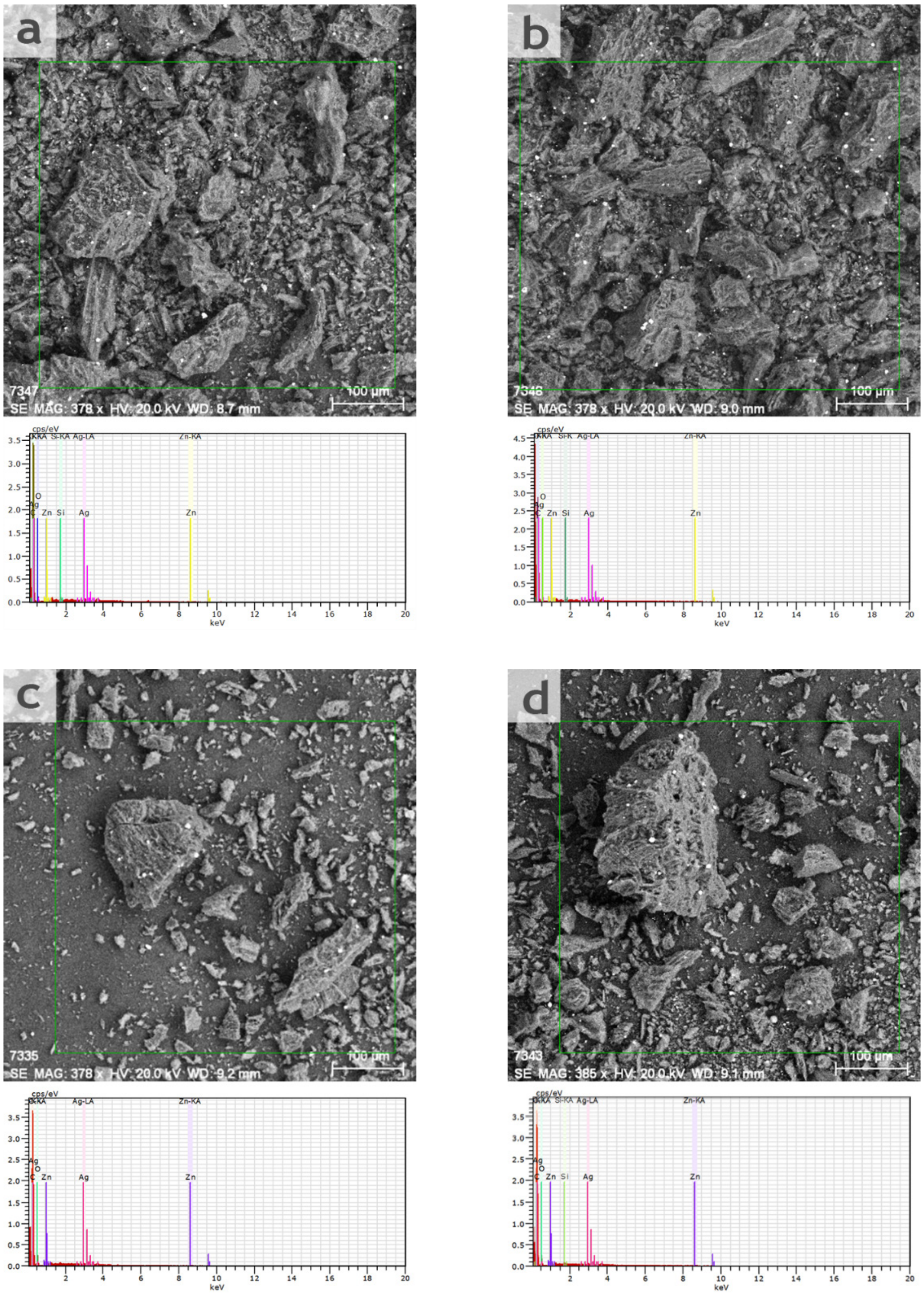

Fig. 9. SEM images and EDX analysis of M1US5 (a), M1TA5 (b), M2US5 (c) and M2TA5 (d).

more often on the surface of the composites obtained via Method 1 (Fig. 9a and 9b) in contrast to Method 2 composites (Fig. 9c and 9d). This observation may be indirect proof of the assumption for silver formation inside the Norit NK pores of M2US5 and M2TA5 since the initial concentration of $AgNO_3$ is the same for all four samples.

Besides silver and carbon, EDX analysis (graphs below the SEM images in Fig. 9 and Fig. 10) indicates the presence of silicon and zinc, which might have left after the carbon activation process. Moreover, these composites show the presence of oxygen, which might be attributed to oxides formed by the Si and Zn impurities in Norit NK as well as the already discussed partial silver oxidation. If the latter is valid then the Ag oxidation seems to occur even before the heating treatment i.e. during the evaporating and/or drying steps.

Samples of the thickened composite's suspensions were collected after the evaporation process to be

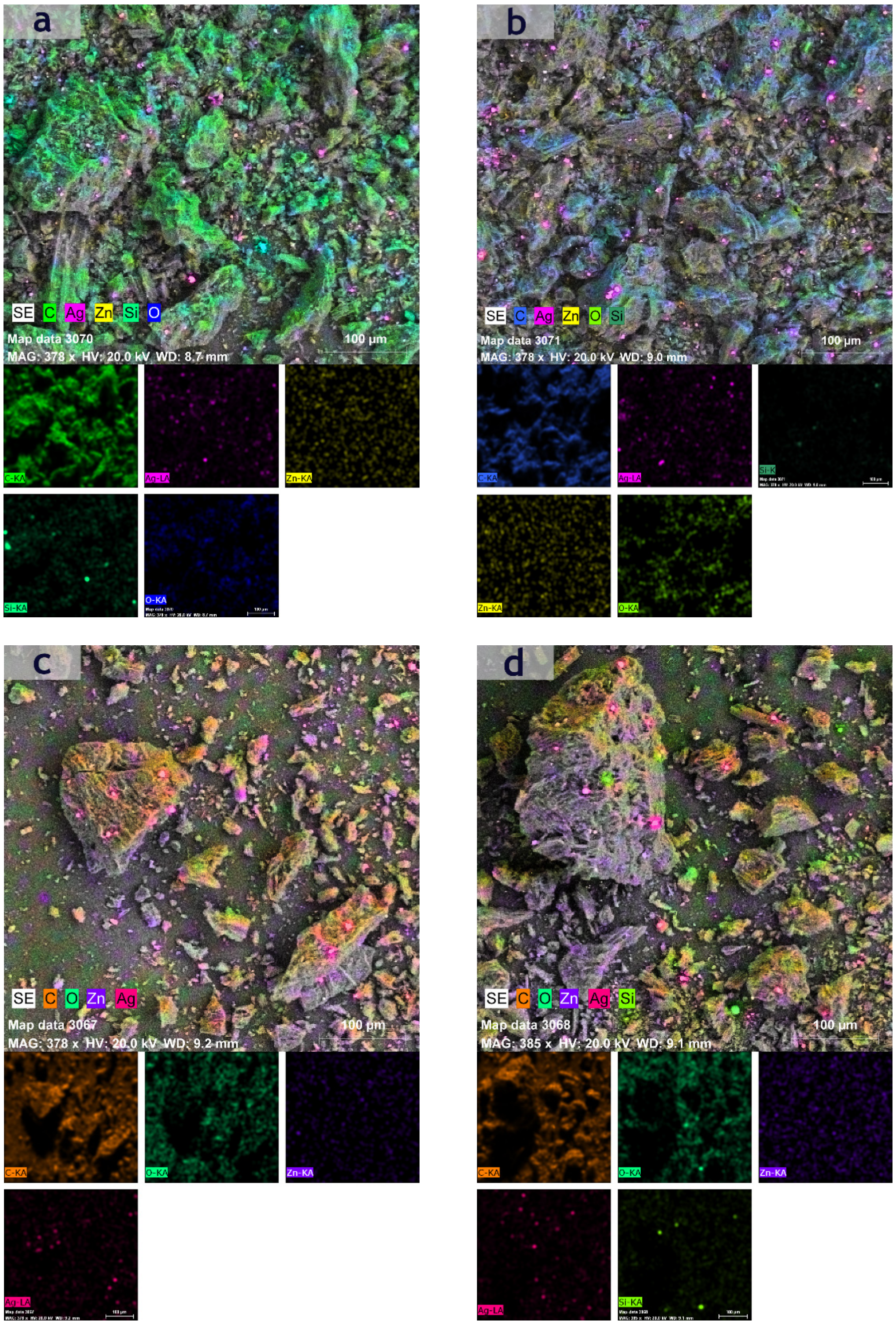

Fig. 10. EDX elemental mapping of M1US5 (a), M1TA5 (b), M2US5 (c) and M2TA5 (d).

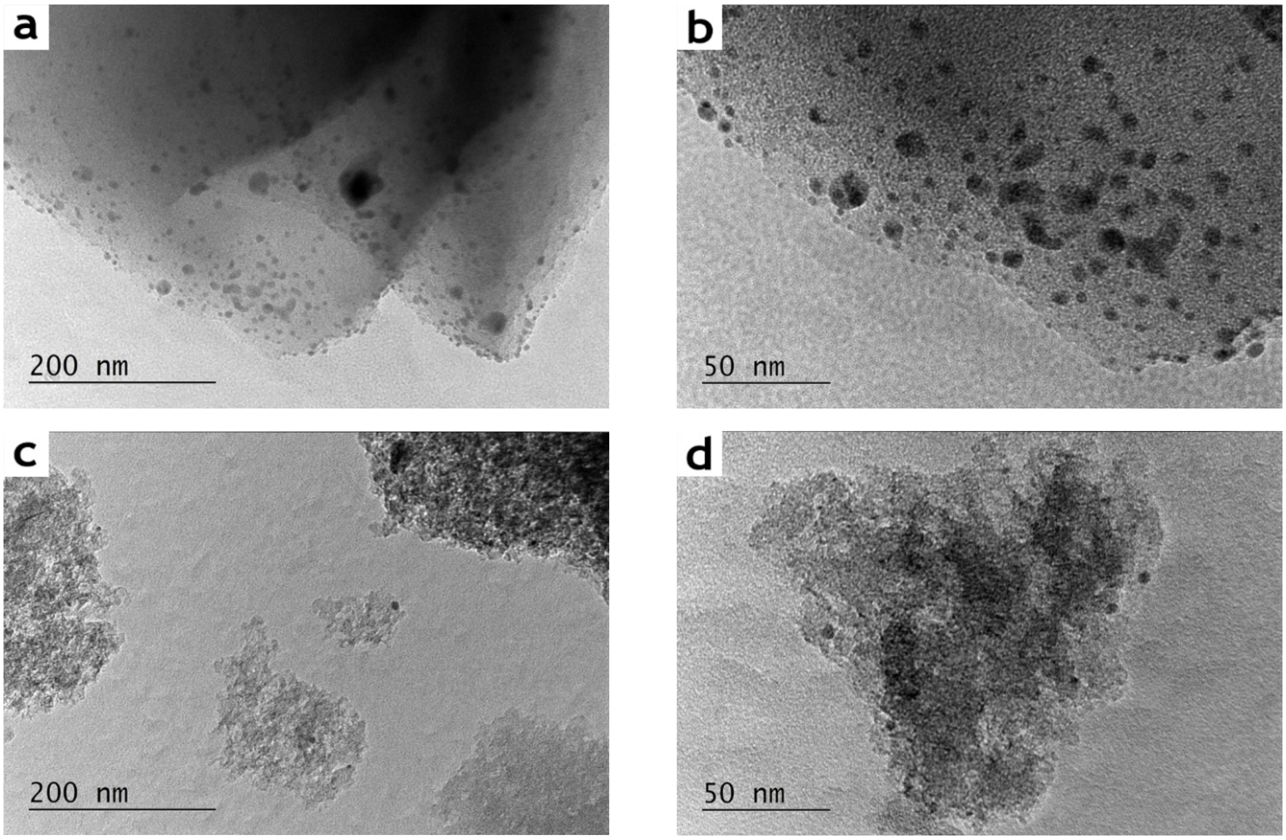

Fig. 11. TEM images of M1US5 (a and b) and M2US5 (c and d) at 40k (a and c) and 100k (b and d) magnifications.

examined by transmission electron microscopy (Fig. 11). These samples were obtained from 5 mmol L^{-1} $AgNO_3$ and Norit NK suspensions, prepared via both methods.

Method 1 composite shows silver nanoparticles attached on the Norit NK particle edges and surface (Fig. 11 a and b). The activated carbon morphology appears to be smooth and layered (Fig. 11a). The Ag particle size is ca. 5 - 20 nm (Fig. 11b). The Norit NK surface seems to be heavily affected in the Method 2 composite case, most likely due to the ultrasonic impact (Fig. 11c and 11d). This is expected to result in a higher surface area, which must have been one of the contributors to the better electrochemical performance of the Method 2 samples. The silver particles are barely noticeable as they were formed mainly inside the pores of the carbon particles (Fig. 11d).

CONCLUSIONS

An ultrasonic approach for synthesis of silver nanoparticles using three different concentrations (4, 5 and 6 mmol L^{-1} of aqueous $AgNO_3$ solution) was developed. Composites of AgNPs and Norit NK activated carbon were prepared via two different methods and then used as a catalytic layer in AGDE. Further, some of the composites were thermally treated under air and argon atmosphere. XRD data show the presence of metal silver and graphite for the samples obtained via Method 1. The graphite reflections are absent in the diffractograms of the Method 2 samples most likely caused by the sonication process. SEM analysis of 5 mM composites obtained via Method 1 and Method 2 presents an additional ongoing agglomeration of the AgNPs during their adsorption on the activated carbon. EDX analysis of M1US5, M1TA5, M2US5 and M2TA5 composites indicates the presence of silicon and zinc impurities as well as oxygen. The oxygen presence might be attributed to silicon and zinc oxides as well as AgNPs oxidation during their adsorption on the carbon and thermal treatment in air.

Among all examined samples, the electrode containing thermally treated composite prepared via Method 2 (M2TA5) seems to exhibit the best electrochemical performance, especially at higher current densities (over 100 mA cm^{-2}). This behaviour could be explained by the activated carbon higher surface area and silver formation inside the carbon pores protecting the Ag from oxidation.

Acknowledgements

In memoriam of our colleague, mentor and friend Prof. Maria Karsheva†

REFERENCES

1. A. Qaseem, F. Chen, X. Wu, R.L. Johnston, Pt-free silver nanoalloy electrocatalysts for oxygen reduction reaction in alkaline media, Catalysis Science & Technology, 6, 2016, 3317-3340.
2. L. Pu, K. Li, Z. Chen, P. Zhang, X. Zhang, Z. Fu, Silver electrodeposition on the activated carbon air cathode for performance improvement in microbial fuel cells, Journal of Power Sources, 268, 2014, 476-481.
3. Y. Yang, Y. Zhou, Particle size effects for oxygen reduction on dispersed silver + carbon electrodes in alkaline solution, Journal of Electroanalytical Chemistry, 397, 1995, 271-278.
4. J. Guo, A. Hsu, D. Chu, R. Chen, Improving oxygen reduction reaction activities on carbon-supported Ag nanoparticles in alkaline solutions, The Journal of Physical Chemistry C, 114, 2010, 4324-4330.
5. S. Salomé, R. Rego, M.C. Oliveira, Development of silver-gas diffusion electrodes for the oxygen reduction reaction by electrodeposition, Materials Chemistry and Physics, 143, 2013, 109-115.
6. T. Wang, M. Kaempgen, P. Nopphawan, G. Wee, S. Mhaisalkar, M. Srinivasan, Silver nanoparticle-decorated carbon nanotubes as bifunctional gas-diffusion electrodes for zinc–air batteries, Journal of Power Sources, 195, 2010, 4350-4355.
7. Y. Cheng, W. Li, X. Fan, J. Liu, W. Xu, C. Yan, Modified multi-walled carbon nanotube/Ag nanoparticle composite catalyst for the oxygen reduction reaction in alkaline solution, Electrochimica Acta, 111, 2013, 635-641.
8. P. Singh, D.A. Buttry, Comparison of oxygen reduction reaction at silver nanoparticles and polycrystalline silver electrodes in alkaline solution, The Journal of Physical Chemistry C, 116, 2012, 10656-10663.
9. N. Furuya, H. Aikawa, Comparative study of oxygen cathodes loaded with Ag and Pt catalysts in chlor-alkali membrane cells, Electrochimica Acta, 45, 2000, 4251-4256.
10. P. Piszczek, A. Radtke, Silver Nanoparticles Fabricated Using Chemical Vapor Deposition and Atomic Layer Deposition Techniques: Properties, Applications and Perspectives: Review, in: M.S. Seehra, A.D. Bristow (Eds.) Noble and Precious Metals - Properties, Nanoscale Effects and Applications, IntechOpen, 2017.
11. G.R. Nasretdinova, R.R. Fazleeva, R.K. Mukhitova, I.R. Nizameev, M.K. Kadirov, A.Y. Ziganshina, V.V. Yanilkin, Electrochemical synthesis of silver nanoparticles in solution, Electrochemistry Communications, 50, 2015, 69-72.
12. M. Starowicz, B. Stypuła, J. Banaś, Electrochemical synthesis of silver nanoparticles, Electrochemistry Communications, 8, 2006, 227-230.
13. J. Zhu, S. Liu, O. Palchik, Y. Koltypin, A. Gedanken, Shape-controlled synthesis of silver nanoparticles by pulse sonoelectrochemical methods, Langmuir, 16, 2000, 6396-6399.
14. R. Sato-Berrú, R. Redón, A. Vázquez-Olmos, J.M. Saniger, Silver nanoparticles synthesized by direct photoreduction of metal salts. Application in surface-enhanced Raman spectroscopy, Journal of Raman Spectroscopy, 40, 2009, 376-380.
15. T. Tsuji, K. Iryo, N. Watanabe, M. Tsuji, Preparation of silver nanoparticles by laser ablation in solution: influence of laser wavelength on particle size, Applied Surface Science, 202, 2002, 80-85.
16. S. Navaladian, B. Viswanathan, T.K. Varadarajan, R.P. Viswanath, Microwave-assisted rapid synthesis of anisotropic Ag nanoparticles by solid state transformation, Nanotechnology, 19, 2008, 045603.
17. C. He, L. Liu, Z. Fang, J. Li, J. Guo, J. Wei, Formation and characterization of silver nanoparticles in aqueous solution via ultrasonic irradiation, Ultrasonics Sonochemistry, 21, 2014, 542-548.
18. Y. Yin, Z. Li, Z. Zhong, B. Gates, Y. Xia, S. Venkateswaran, Synthesis and characterization of stable aqueous dispersions of silver nanoparticles through the Tollens process, Journal of Materials Chemistry, 12, 2002, 522-527.

19. M. Jose, M. Sakthivel, Synthesis and characterization of silver nanospheres in mixed surfactant solution, Materials Letters, 117, 2014, 78-81.
20. Z. Zaheer, Rafiuddin, Multi-branched flower-like silver nanoparticles: Preparation and characterization, Colloids and Surfaces A: Physicochemical and Engineering Aspects, 384, 2011, 427-431.
21. S. Pyne, S. Samanta, A. Misra, Photochemical synthesis of Ag nanobars and their potential application as catalyst, Solid State Sciences, 26, 2013, 1-8.
22. A.R. Siekkinen, J.M. McLellan, J. Chen, Y. Xia, Rapid synthesis of small silver nanocubes by mediating polyol reduction with a trace amount of sodium sulfide or sodium hydrosulfide, Chemical Physics Letters, 432, 2006, 491-496.
23. G.M. Raghavendra, J. Jung, D. Kim, K. Varaprasad, J. Seo, Identification of silver cubic structures during ultrasonication of chitosan $AgNO_3$ solution, Carbohydrate Polymers, 152, 2016, 558-565.
24. J.S. Kim, E. Kuk, K.N. Yu, J.-H. Kim, S.J. Park, H.J. Lee, S.H. Kim, Y.K. Park, Y.H. Park, C.-Y. Hwang, Y.-K. Kim, Y.-S. Lee, D.H. Jeong, M.-H. Cho, Antimicrobial effects of silver nanoparticles, Nanomedicine: Nanotechnology, Biology and Medicine, 3, 2007, 95-101.
25. N.D. Trinh, T.T.B. Nguyen, T.H. Nguyen, Preparation and characterization of silver chloride nanoparticles as an antibacterial agent, Advances in Natural Sciences: Nanoscience and Nanotechnology, 6, 2015, 045011.
26. A. Pal, S. Shah, S. Devi, Microwave-assisted synthesis of silver nanoparticles using ethanol as a reducing agent, Materials Chemistry and Physics, 114, 2009, 530-532.
27. N.G. Bastús, F. Merkoçi, J. Piella, V. Puntes, Synthesis of highly monodisperse citrate-stabilized silver nanoparticles of up to 200 nm: Kinetic control and catalytic properties, Chemistry of Materials, 26, 2014, 2836-2846.
28. F.P. Mehr, M. Khanjani, P. Vatani, Synthesis of Nano-Ag particles using sodium borohydride, Oriental Journal of Chemistry, 31, 2015.
29. Y. Qin, X. Ji, J. Jing, H. Liu, H. Wu, W. Yang, Size control over spherical silver nanoparticles by ascorbic acid reduction, Colloids and Surfaces A: Physicochemical and Engineering Aspects, 372, 2010, 172-176.
30. H. Xu, B.W. Zeiger, K.S. Suslick, Sonochemical synthesis of nanomaterials, Chemical Society Reviews, 42, 2013, 2555-2567.
31. E.B. Budevski, I.D. Iliev, A.R. Kaisheva, S.S. Gamburtzev, E.B. Budevski, E.B. Vakanova, Method for producing powdered wetproofed material useful in making gas-diffusion electrodes. U.S. Patent No. 4,031,033. Patent and Trademark Office, Washington, United States, 1977.
32. J. Christian, J. Spreadborough, Transactions of the Metallurgical Society of Aime, 233, 1965, 1182-1183 (ICSD 44387).
33. U. Hofmann, D. Wilm, Über die kristallstruktur von kohlenstoff, Zeitschrift für elektrochemie und angewandte physikalische chemie, Verlag Chemie, 42, 1936, 504-522.